Received: 4 December 2020 | Accepted: 21 December 2020

DOI: 10.1002/prp2.716

ORIGINAL ARTICLE

Elimination of macrophages reduces glutaraldehyde-fixed porcine heart valve degeneration in mice subdermal model

Zongtao Liu | Yixuan Wang | Fei Xie | Xing Liu | Fei Li | Nianguo Dong

Department of Cardiovascular Surgery, Union Hospital, Tongji Medical College, Huazhong University of Science and Technology, Wuhan, China

Correspondence
Fei Li and Nianguo Dong, Department of Cardiovascular Surgery, Union Hospital, Tongji Medical College, Huazhong University of Science and Technology, 1277, Wuhan Jiefang Road, Jianghan District, Wuhan, 430022, China.
Email: lifei_union@sina.com (F. L.) and 1986xh0694@hust.edu.cn (N. D.)

Funding information
National Natural Science Foundation of China, Grant/Award Number: 82001701; National Key Research and Development Program, Grant/Award Number: 2016YFA0101100

Abstract

Glutaraldehyde-fixed porcine heart valve (GPHV) calcify and deteriorate over time. The aim of this study was to explore the roles macrophages play in mediating calcification and degeneration of the valve's connective tissue matrix. GPHV were implanted subcutaneously in the abdomens of C57BL/6 mice. The mice were equally divided into two study groups: (a) GPHV +phosphate buffered saline (PBS) liposomes, and (b) GPHV +clodronate liposomes. GPHV were collected for further analyses at 4 weeks post implant. Macrophages were almost depleted from the spleens of mice injected with clodronate liposomes as indicated by immunohistochemical staining. Furthermore, the expression of matrix metalloproteinase-2 (MMP-2), MMP-9, and pro-inflammatory cytokines like IL-1β, IL-6, MCP-1, MIP-1a, MIP-1b, were downregulated in the GPHV +Clodronate liposomal group compared with the GPHV+PBS liposomal group. Clodronate liposomal treatment led to significant decreases in the expression of RUNX2, ALP and OPN as well as less calcium deposits in GPHVs compared with PBS liposomal treatment. This finding indicated that infiltrating macrophages are critically involved in the development of calcification and deterioration in GPHVs. Macrophage depletion by clodronate liposomes decreased the extent of GPHV's calcification and deterioration.

KEYWORDS
Clodronate liposomes, Glutaraldehyde-fixed porcine heart valve, macrophage, metalloproteinase, structural valve degeneration

1 | INTRODUCTION

Surgical therapy for valvular heart disease accounts for 20% heart surgery. Nowadays, there are more than 250 000 heart valve replacements each year worldwide.[1] Either mechanical valve or glutaraldehyde-fixed bioprosthetic heart valve (GBHV) is widely used. The latter have porcine or bovine origins, and can be used for the replacement of diseased valve. Mechanical valve requires lifelong anticoagulation treatments,

Abbreviations: ALP, Alkaline phophatase; BSA, Bovine serum albumin; DAPI, 4'6'-diamidino-2-phenylindole; DW, Dry weight; FITC, Fluorescein isothiocyanate; GAPDH, Glyceraldehyde 3-phosphate dehydrogenase; G-CSF, Granulocyte colony-stimulating factor; GM-CSF, Granulocyte-macrophage colony-stimulating factor; GPHVs, Glutaraldehyde-fixed porcine heart valve; H&E, Hematoxylin and eosin; I.P., Intraperitoneal; IFN-g, Interferon gamma; IL, Interleukin; MCP, Monocyte chemoattractant protein; MIP, Macrophage inflammatory protein; MMP-2, Matrix metalloprotein-2; mRNA, Messenger RNA; OPN, Osteopontin; PBS, Phosphate buffer saline; qRT-PCR, Quantitative reverse transcription polymerase chain reaction; RANTES, Regulated upon activation, normal T cell expressed and presumably secreted; RNA, Ribonucleic acid; SD, Standard deviation; SVD, Structural valve degeneration; TNF, Tumor necrosis factor.

Zongtao Liu and Yixuan Wang contributed equally to this work.

but is durable. The application scope of bioprosthetic valve, including TAVR, though exhibiting excellent hemodynamic performances, is still limited due to the early degeneration.[2,3] Although progress has been accomplished in the fixation, pre-implantation, and anti-calcification treatment of GBHV, structural valve degeneration (SVD) remains an important limitation of this type of prosthesis.[4]

In 2000, researchers examined the failed explanted heart valve from patients who had either received a GBHV or a valve synthesized from autologous pericardium treated with glutaraldehyde. The GBHV demonstrated large areas of calcification and inflammation owing to the macrophage infiltration.[5] Macrophages constitute an important part of the innate immune system and can transform to foam cells that in turn produce and release inflammatory cytokines and matrix metalloproteinase (MMP) production that accelerates GBHV calcification.[6] Amount of clinical and experimental projects have shown that MMPs play similiar roles in the calcification of native and bioprosthetic heart valve. Recently, a broad spectrum of clinicopathologic studies indicated that hyaline cartilage tissue represented an early stage of endochondral ossification within the aortic valve leaflets. Subject to these circumstances, a significant number of MMPs were immunohistochemically expressed,[7] including the upregulation of MMP-1, -2, -3, -7, -9, -12, and -13, in calcified aortic valve disease, that may mediate tissue remodeling in aortic valve.[8-10] At the same time, the bioprosthetic heart valve failure was associated with increased levels of MMP-9 and MMP-2.[6,11]

Clodronates have been shown to have anti-atherosclerotic effects based on the inhibition of aortic calcification by reducing lipid accumulation and fibrosis, and decreasing pre-established atherosclerotic lesions.[12] Moreover, Clodronate encapsulated into liposomes could also reduce neo-intimal proliferation after balloon injury in rats and hypercholesterolemic rabbits.[12,13] Based on these reported observations, we hypothesized that the infiltration of peripheral macrophages was possibly detrimental for GBHV in vivo, and macrophage elimination could prevent GBHV calcification and degradation.

2 | MATERIALS AND METHODS

2.1 | Dissection of porcine aortic valve leaflets

Hearts of adult pigs (weights ranging from 120 to 150 kg) were obtained from a local abattoir, transferred to the laboratory in cold isotonic saline, and processed immediately. Within 1 h after euthanasia, aortic valve leaflets were dissected precisely from the aortic root and rinsed with cold isotonic saline under aseptic conditions. The valve leaflets were then incubated with Dulbecco's modified eagle's medium (Gibco) that contained antibiotics (100 U/ml penicillin, 100 mg/ml streptomycin, and 250 mg/ml amphotericin B) at 4°C overnight, fixed in 0.6% glutaraldehyde for 48 h, and were then thoroughly rinsed in saline before operation. The glutaraldehyde concentration and time allotted were respectively similar with those used and required in the clinical setting for bioprosthetic heart valve for human patients.[14]

2.2 | Animals

Male C57BL/6 mice (eight weeks old, body weight 20–22 g) were studied. The mice were purchased from the Tongji Medical College Laboratory Animal Center, and were kept in groups of six in cages in controlled environmental and relative humidity (RH) conditions (22–24°C, RH: 50%–60%). Standard rodent diet and tap water were accessible to mice ad libitum. In addition. The mice were randomly divided into two separate groups.

2.3 | Surgical procedures

A previously described, a mice subdermal implantation model was used.[15] Prior to surgery, the mice were induced and maintained with isoflurane. The abdomens of the animals were shaved, disinfected with sterile gauzes soaked with iodine solution, and covered with surgical sheets. A small midline incision was made, and a ventral midline subcutaneous pocket was created using blunt dissection. A tissue graft (1 cm^2) was placed in the subcutaneous pocket and secured under the surface of the skin with 4-0 prolene sutures. The incision was then closed with 4-0 absorbable sutures and cleaned with betadine. The animals were placed on a heating pad to recover from anesthesia, and were then returned to their housing units. The surgical site was evaluated daily for signs of swelling or infection. The dietary habits and general health profiles of the animals were recorded daily. Four weeks after surgery, animals were euthanized with an intraperitoneal administration of an overdose of pentobarbital sodium. Samples were retrieved and divided into two groups.

2.4 | Drug treatment

In the preliminary experiments, different dosages and routes of administration of clodronate liposomes were evaluated based on previously described protocols.[16] All animals received the substance intraperitoneally (i.p.). One day before the operations, animals were randomly divided into control and treatment groups. Mice in the treatment group received clodronate liposomes (200 µl per mice), whereas mice in the control group received PBS liposomes (200 µl per mice). The control group was studied to exclude possible effects exerted by liposomes that were independent of clodronate. As shown in Figure 1, the surgical operations were conducted on the day after the first clodronate liposomal administration. The administration of clodronate liposomes was given at day 2, day 5, day 8 and day 11 after subcutaneous implant

2.5 | Immunohistochemical analyses

All tissues were fixed in 4% paraformaldehyde for 48 h, dehydrated, and subsequently embedded in paraffin. Tissue samples were stained with hematoxylin and eosin (H&E) to depict the matrix and cellular architecture. Masson's trichrome was also used for the assessment

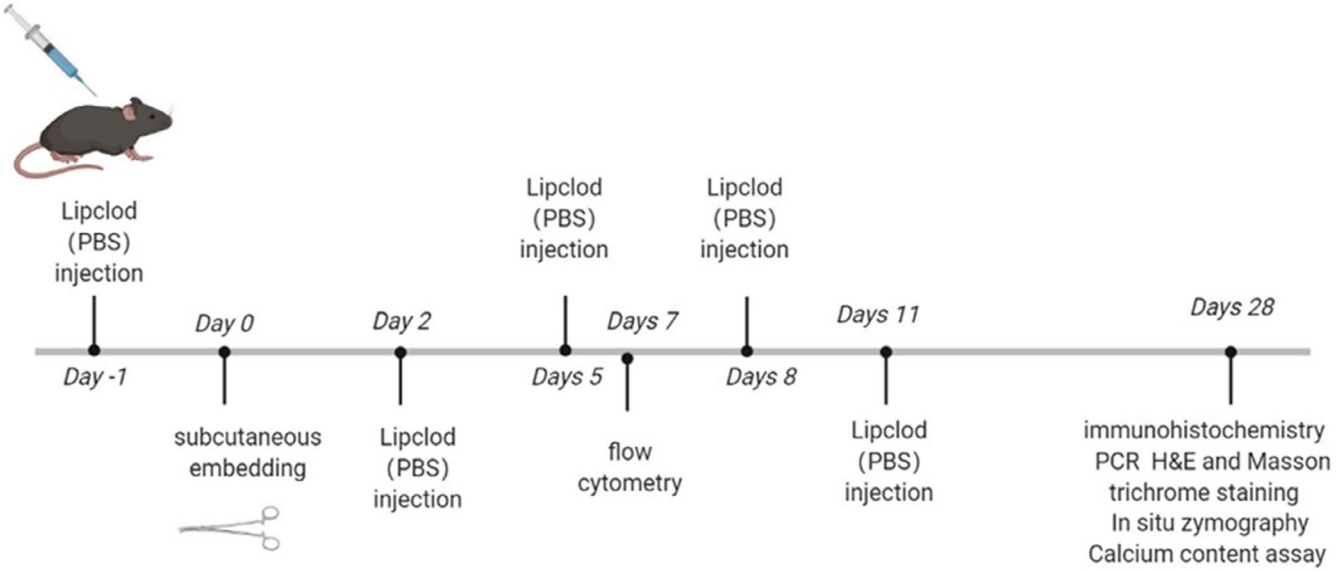

FIGURE 1 Experimental protocol. For details, see the Methods section. Groups of mice were either treated with PBS or clodronate liposomes. Surgical operations were conducted one day after the first administration of clodronate liposomes (or PBS liposomes). The administration of clodronate liposomes (or PBS liposomes) was done at day 2, day 5, day 8 and day 11 after subcutaneous implant. After 4 weeks, glutaraldehyde-fixed porcine heart valve (GPHV) and spleen tissue were collected for further analysis (Lipclod = clodronate liposomes, PBS = phosphate buffered saline)

of gross collagen and elastin organization and histological evaluation of the ECM. Immunohistochemistry was performed to detect F4/80 (Abcam, ab6640, 1:100), RUNX2 (Abcam, ab192256, 1:200) and ALP (ZEN BIO, 381009, 1:100), OPN (Abcam, ab8448, 1:200). Briefly, after dehydration, sections were boiled for 2 min in citrate buffer (pH 6.0) for antigen retrieval, followed by treatment with 3% H_2O_2 to block endogenous peroxidase activity. Subsequently, the sections were incubated overnight at 4°C with primary antibodies. Followed by incubation with an appropriate second antibody for 30 min at room temperature. DAB (diaminobenzidine) was used as a substrate for staining. Image-Pro Plus was used for quantitative analyses. To quantify levels of target molecular expression, positively stained tissues were calculated in a minimum of five random microscopic fields.

2.6 | Immunofluorescence staining

Immunofluorescence staining was performed with the use of F4/80 (Abcam, ab6640, 1:100 dilution), CD3 (Abcam, ab135372, 1:100 dilution) primary antibodies, and labeled with the 488 anti-rat (Aspen, AS-1110, 1:50 dilution) and CY3 anti-rabbit (Aspen, AS-1110, 1:50 dilution) secondary antibodies in a dark humid chamber at 4°C for 1 h. Nuclei were stained with 4′6′-diamidino-2-phenylindole (DAPI) (Life Technologies, 1:1000 dilution). Tissue sections were imaged with a confocal microscopy system (Carl Zeiss LSM700), and the software ZEN (Carl Zeiss) was used for image analysis. To quantify levels of target cell types, positively stained cells were counted in a minimum of five random microscopic fields, and the proportion of the double positive cells was calculated and presented.

2.7 | Spleen cell isolation and flow cytometry

Flow cytometry was performed on the spleen samples of mice which was used to monitor the removal efficiency of macrophages in a separate experiment different from GBHV embedding collected on day 7 after the surgical procedure. The mice were deeply anesthetized and the spleens were removed and collected in a 1.5 ml tube. To obtain a single-cell suspension, the spleens were grinded in PBS based on a mechanical trituration method, and were then filtered through a 100 μm cell strainer. The cell suspension was centrifuged for 10 min at 500 *g* at 4°C, and the supernatant was discarded. Red blood cells were removed following the resuspension of the cells in red blood cell lysis buffer for 30 s. The cell suspension was then centrifuged again for 10 min at 500 *g* at 4°C and the supernatant was discarded. After washing in PBS, the cells were resuspended in 1 ml of PBS. A Single-cell suspension of 100 μl was incubated with fluorescence-conjugated rat anti-mouse fluorescein isothiocyanate (FITC) F4/80 (1:100, BioLegend) for 1 h at 4°C. The cells were then centrifuged for 10 min at 500 *g* at 4°C. After the supernatant was discarded, the cells were washed once with PBS. The cells were then resuspended in 200 μl PBS and analyzed by flow cytometry (BD Biosciences).

2.8 | Determination of cytokines in glutaraldehyde-fixed porcine heart valve with Bio-Plex assays

GPHV was procured at day 28 after embedding, 100 mg of tissue was put into a 1 ml EP tube. Then pre-cooled protein extraction reagent was added, with tissue homogenizeded at a low speed for 30 s

using a homogenizer, followed by 1 min ice bath process until the tissue was completely decomposed. Then the liquid was centrifuged at 4000 *g* for 15 min, and the supernatant was collected and placed in tube.

The concentrations of cytokines were determined using the Bio-Plex mouse cytokine panel. Plates were read on a Bio-Plex Array Reader (Bio-Plex 200 System using the Bio-Plex Manager software, Version 4.0, Bio-Rad Laboratories), according to the manufacturer's instructions. The concentrations of 19 cytokines [granulocyte colony-stimulating factor (G-CSF), granulocyte-macrophage colony-stimulating factor (GM-CSF), interferon gamma (IFN-γ), interleukin (IL)-1a, IL-1b, IL-2, IL-3, IL-4, IL-5, IL-6, IL-9, IL-10, IL-13, IL-17, monocyte chemoattractant protein (MCP)-1, macrophage inflammatory protein (MIP)-1a, MIP-1b, regulated upon activation, normal T cell expressed and presumably secreted (RANTES), and tumor necrosis factor (TNF)-α] were determined.

2.9 | Quantitative reverse transcription polymerase chain reaction (qRT-PCR)

Total ribonucleic acid (RNA) was extracted from glutaraldehyde-fixed porcine heart valve by using RNAiso Plus (Takara) according to the manufacturer's instructions. Reverse transcription of RNA was performed using PrimeScript™ RT Master Mix (Takara). Quantitative real-time PCR was performed with SYBR_Premix Ex Taq™ (Takara) on a StepOnePlus™ RT-PCR System (Applied Biosystems). The primers for mouse target genes are listed in Table 1. All PCRs were performed in duplicate, and messenger RNA (mRNA)-fold changes were calculated by the 2−ΔΔCt method using glyceraldehyde 3-phosphate dehydrogenase (GAPDH) as the internal reference.

2.10 | In situ zymography for the determination of MMP activity

Frozen sections (thickness of 7 μm) of the embedded GPHV were procured at day 28. Tissue sections were incubated with 40 μmol DQ gelatin (Invitrogen) for 2 h, and fluorescence was measured by laser scanning confocal microscopy without washing. Fluorescent images were analyzed with the software Image-Pro.

TABLE 1 Sequences (5′-3′) of primers and probes (the letter R denotes "reverse," while F denotes "forward")

RUNX2 F	AACTTGCTAACGTGAATGGTC
RUNX2 R	GGTTCAAAGAAGTCACCCGAT
GAPDH F	CCAGCCTCGTCCCGTAGA
GAPDH R	TAAGTTGCCGTGTCAGTTCC
MMP-2 F	ACACCTACACCAAGAACTTCCG
MMP-2 R	CCAAATAAACCGCCTGTCAC
MMP-9 F	AAAGACGACATAGACGGCATCC
MMP-9 R	GGTGGTGTTGACTTGGTGTCG

2.11 | Calcium content assay

Explanted samples were weighed, frozen at −80°C for 1 h, and lyophilized for 36 h. Subsequently, dry weight (DW) was obtained. External connective tissue was removed and the samples dried in an oven at 70°C for 72 h. The dried samples weighed 20 mg and the calcium content of the dried samples was extracted in 1 ml of 50% nitric acid. Extractable calcium content per DW was measured by atomic absorption spectrophotometry (SpectrAA-240FS, Palo Alto).

2.12 | Statistics

Continuous data were expressed as mean ± standard deviation (SD), and $p < .05$ was considered as statistically significant. Data were compared with Student's *t*-tests. Statistical analysis was carried out with the software GraphPad Prism 6.

3 | RESULTS

3.1 | Elimination of macrophages based on clodronate liposomal treatment

To deplete peripheral macrophages, mice were injected with clodronate liposomes. Seven days after injection, 80% of $F4/80^+$ macrophages were removed from the spleen in the clodronate liposome-treated mice compared with control mice (Figure 2A,B). This result also suggested the success of the depletion of macrophages. Animals that received clodronate liposomes showed no visible disorders, such as infection, reduced appetite, or inhibition of motor activity. The weight of mice was 22–24 g after 4-week observation. At 28 days after implant, we used immunohistochemical staining to determine whether $F4/80^+$ macrophages were depleted, and found that the expression of $F4/80^+$ macrophages was markedly decreased in the spleen in the clodronate liposome-treated mice compared with control mice (Figure 2C,D).

3.2 | Biocompatibility in mouse subdermal model

The implanted valve leaflets and the surrounding tissues were analyzed by H&E and Masson's trichrome staining (Figure 3A,B). After a four-week implantation period, the implanted valve leaflets in the PBS liposome-treated mice were presented with a dense fibrous capsule formation, a high level of scaffold degradation, and a dense infiltration of inflammatory cells around the implantation site. The implanted valve leaflets in the Clodronate liposome-treated mice

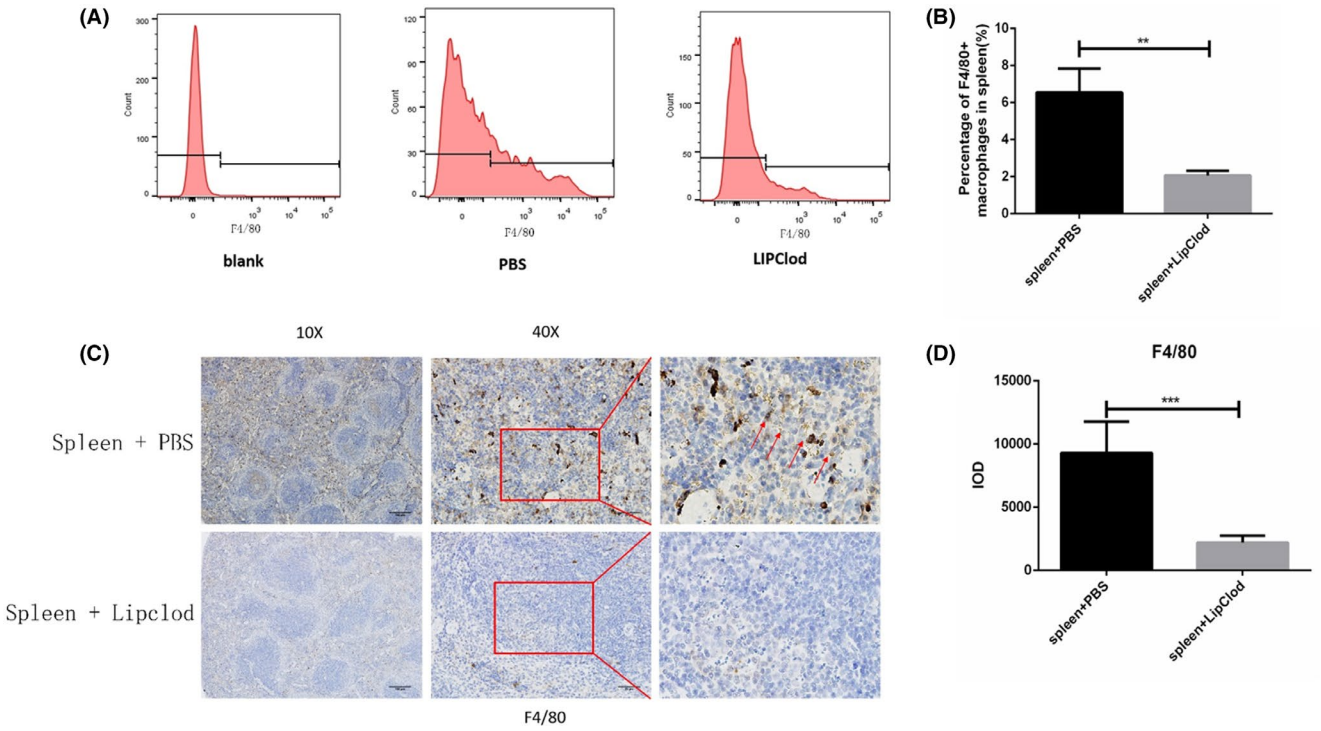

FIGURE 2 Macrophages were removed from spleen under clodronate liposome treatment. (A) Flow cytometric analysis shows the percentage of F4/80$^+$ macrophages in the spleen of blank (non-staining), PBS, and Lipclod groups at 7 days after surgical operations. (B) Bar graph shows the quantification of the percentage of F4/80$^+$ macrophages in the spleen of blank, PBS, and Lipclod groups. (C, D) Representative images of F4/80$^+$ immunohistochemical staining and quantification data showing that liposome treatment significantly decreases the infiltration of macrophages in mice spleens compared with PBS liposomes (data are mean ± standard deviation (SD), n = 5 per group, $^*p < .05$; $^{**}p < .01$; $^{***}p < .001$)

exhibited a thick fibrous capsule formation, seldom scaffold degradation, and a decreased infiltration of inflammatory cells within the implants which was indicative of a moderate chronic inflammatory response. As shown in Figure 3C, the implanted valve leaflets in the PBS liposome-treated mice exhibited a statistically significant decrease in the fibrous capsule thickness compared with valve leaflets in the clodronate liposome-treated mice. Figure 3D shows that the implanted valve leaflets in the clodronate liposome-treated mice significantly reduced the inflammatory response compared with the valve leaflets in the PBS liposome-treated mice. The number of inflammatory cells observed in the implanted valve leaflets in the Clodronate liposome-treated mice was significantly less than in valve leaflets in the PBS liposome-treated mice.

3.3 | Subcutaneous clodronate treatment mice showed significantly reduced number of F4/80$^+$ macrophages, CD3$^+$ T-cell numbers, and inflammatory factor production in GPHVs

As shown in Figure 4A,D, the implanted valve leaflets in the clodronate liposome-treated mice showed significantly reduced number of F4/80$^+$ macrophages and CD3$^+$ T-cell infiltration compared with the valve leaflets in the PBS liposome-treated mice. Further, the implanted valve leaflets were analyzed using the Bio-Plex assay to assess the presence and quantify the concentration of 19 cytokines [G-CSF, GM-CSF, IFN-g, IL-1a, IL-1b, IL-2, IL-3, IL-4, IL-5, IL-6, IL-9, IL-10, IL-13, IL-17, MCP-1, MIP-1a, MIP-1b, RANTES, and TNF-a]. As shown in Figure 4E, the levels of macrophage-related cytokines IL-1a, IL-1b, IL-6, MCP-1, MIP-1a, MIP-1b, and T cell-related cytokines IL-17A, RANTES in the GPHVs of clodronate liposome-treated mice were significantly lower than the GPHVs of PBS liposome-treated mice which was consistent with previous immunofluorescence findings.

3.4 | Macrophage depletion leads to decreased MMP activity and mRNA expression

MMP which were secreted by macrophages could play central roles in ECM (extracellular matrix) remodeling. The MMP activity level measured with in situ zymography showed significant increases in the GPHVs of PBS liposome-treated mice compared with the GPHVs of clodronate liposome-treated mice (Figure 5A,B). At the same time, as shown in Figure 5C,D, the GPHV of the clodronate liposome-treated mice revealed a significant decrease in the mRNA expression of MMP-2 and MMP-9, compared with the GPHVs of PBS liposome-treated mice.

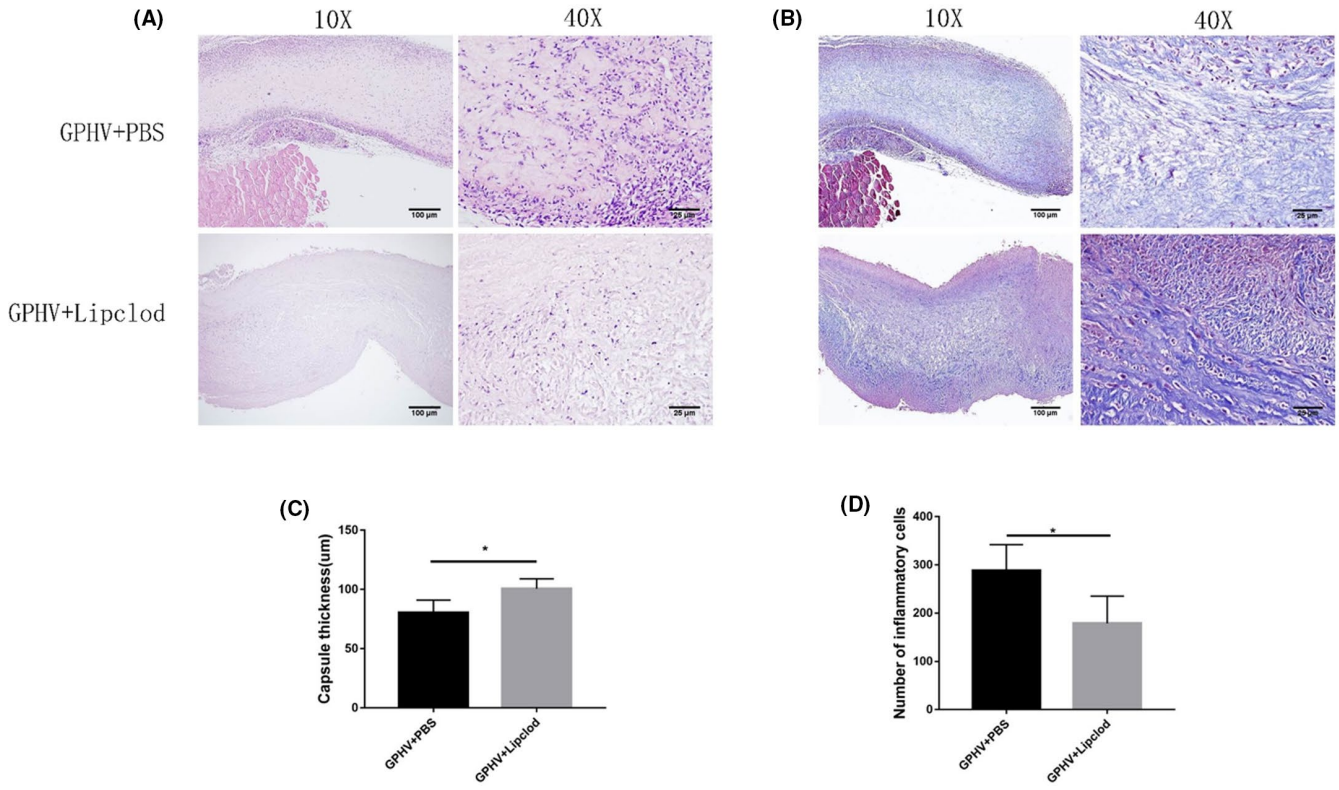

FIGURE 3 Histological characterization of host response tendency of GPHV in vivo implantation in a mouse subdermal model for a period of 4 weeks. (A, B) Representative images of H&E and Masson trichrome staining of the implanted valve leaflets and the surrounding tissues. (C) Thickness of the fibrous capsule formed around the implanted valve leaflets. (D) Number of inflammatory cells observed in the implanted valve leaflets after retrieval (data are mean ± SD $n = 5$ per group, $^{*}p < .05$; $^{**}p < .01$; $^{***}p < .001$)

3.5 | Reduction of osteoblast differentiation attributed to macrophage depletion

ECM remodeling and degradation was the first step of GPHV degeneration, followed by osteoblast differentiation. To evaluate if clodronate liposome treatment affected the osteoblast differentiation in GPHVs, immunohistochemical staining of the osteoblast transcription factor RUNX2 and ALP OPN was confirmed less frequently than in GPHVs treated with PBS liposomes (Figure 6A,B, Supplementary material). Moreover, as shown in Figure 6C, the GPHV of clodronate liposome-treated mice revealed a significant decrease in the mRNA expression of Runx2 compared with the GPHV of the PBS liposome-treated mice. The calcium contents of explanted tissues are shown in Figure 6D. The calcium deposition level of GPHV in clodronate liposome-treated mice was significantly lower than that in PBS liposome-treated mice.

4 | DISCUSSION

Epidemiological and experimental studies have shown that aortic valve stenosis and GBHV degeneration had similiar pathological process. Among them was the accumulation of lipids and inflammatory cells, including macrophages and T cells in the sub-endothelium. The continuous release of cytokines and MMP production would further cause immune injury in the case of GBHV, and cholesterol (CH) crystals and calcium deposits would be formed at the end-stages of the disease.[17-19] It is well known that activated macrophages produce and release MMPs.[20] Substrates for MMP-9 include among others collagen type I, elastin, and fibronectin.[21] Experimental studies that the presence of fragmented collagen along with macrophages presentation near GBHV futher verify the fact that activated macrophages participating in the matrix degradation of GBHV.[6] However, the process of bioprosthetic heart valve implantation is a type of xenotransplantation. This evokes a vigorous immune responses. It is generally accepted that the glutaraldehyde-fixed heart valve reduces the immunogenicity of bioprosthetic valve via the crosslinking process.[22,23] Unfortunately, the calcification of bioprosthetic valve occurs on account of chemical processes between free aldehyde groups, phospholipids, and other components with calcium ions in the circulation.[24]

Meanwhile, macrophages against xenoantigens have been manifested to play a crucial role in the bioprosthetic heart valve calcification.[25] Some investigators have evaluated the role of the macrophages in the failure of bioprosthetic valve. Certain groups have studied animal models, and observed the macrophage responses in vivo or in vitro, and found evidence suggestive of an immune system response to GBHV.[26,27] The administration of liposome-encapsulated clodronate is one of the most efficient methods to systemically deplete macrophages. Free clodronate is not a toxic

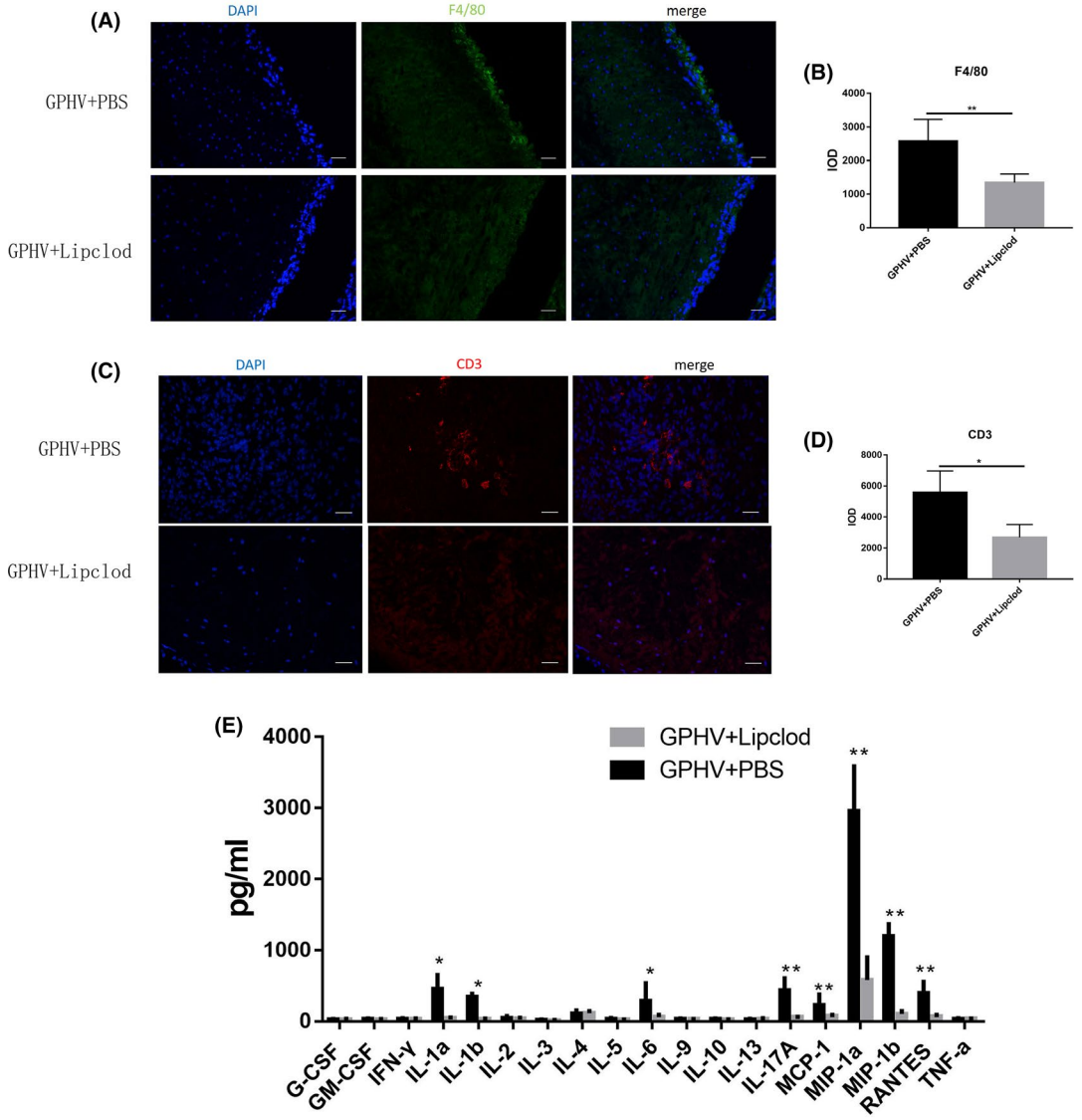

FIGURE 4 Clodronate liposome treatment reduced the number of F4/80$^+$ macrophages, CD3$^+$ T-cell infiltration, and the production of inflammatory factor in the GPHVs after surgical operations. (A) Representative images of F4/80$^+$ macrophages (green) of the GPHV in PBS and Lipclod groups 28 days after surgical operations. (B) Quantification data show that the liposomal treatment significantly decreased the macrophage infiltration of the GPHV Lipclod groups compared with the PBS groups. (C) Representative images of CD3$^+$ T cell (red) of the GPHV+PBS and the GPHV+Lipclod groups at 28 days after surgical operations. (D) Quantification data show that liposomal treatment significantly decreased the CD3$^+$ T-cell infiltration of the GPHV+Lipclod groups compared with the PBS groups. (E) Quantification data show that liposomal treatment significantly decreases the infiltration of inflammatory factors in the case of the GPHV+Lipclod group compared with the GPHV+PBS group (data are mean ± SD, n = 5 per group; *p < .05; **p < .01; ***p < .001)

drug, and is not easily transported through cell membranes, whereas clodronate liposomes are recognized as foreign particles and are rapidly phagocytosed by macrophages.[28,29]

In this study, we found that macrophage depletion prevented structural valve degeneration for 28 days after surgical operations. This process may occur in two main ways. First, the depletion of macrophages will lead to a diminished CD3$^+$ T-cell activation, and would thus reduce T-cell infiltration to the GBHV. Upon activation, quiescent T cells can differentiate into cytotoxic T cells that directly mediate valve degradation. Meanwhile, they can also secrete proinflammatory cytokines, like IFN-g, IL-1a, IL-1b, IL-2, IL-3, IL-4, IL-5, IL-6, IL-9, IL-10, IL-13, IL-17, MCP-1, MIP-1a, MIP-1b, RANTES, and TNF-a, that will initiate a downstream inflammatory cascade. Second, MMP-2 and MMP-9 secreted by macrophages were also reduced, and lead to a diminished degradation of the valve. MMP-2 and MMP-9 are known to bind to insoluble elastin. This binding process is considered as the first step in elastin degradation. This verifies that MMP-2 and MMP-9 could take an active part in elastin degradation and calcification. Manuela Voinea Calin has also reported that depletion of macrophages could decrease the expression of IL-1β and MMP activities in hyperlipemic hamsters heart valve,[25] which was in consistent with our research, however, further in vivo studies focusing on peri-GPHV tissues and inflammation indicators were needed to

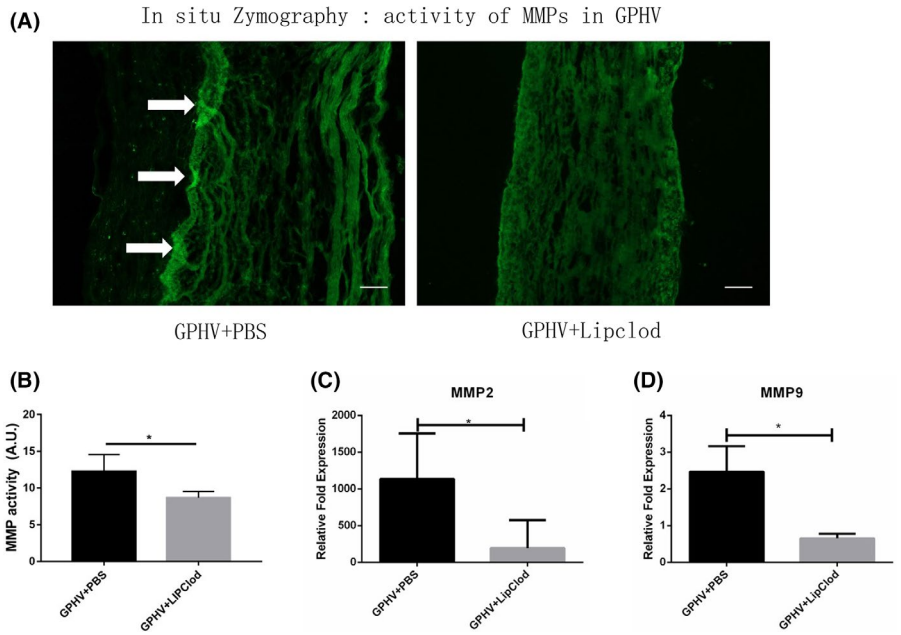

FIGURE 5 In situ zymography shows the activities of metalloproteinases (MMPs) in GPHV. (A) In situ zymography of GPHV showing decreased MMP activity in the GPHV+Lipclod group that was mitigated by the Lipclod treatment. Green fluorescence indicates active MMP. (B) Graphical presentation of MMP activity. (C) Messenger ribonucleic acid (mRNA) expression levels of MMP-2 and (D) MMP-9 that varied between groups (data are mean ± SD, $n = 5$ per group, $^{*}p < .05$; $^{**}p < .01$; $^{***}p < .001$)

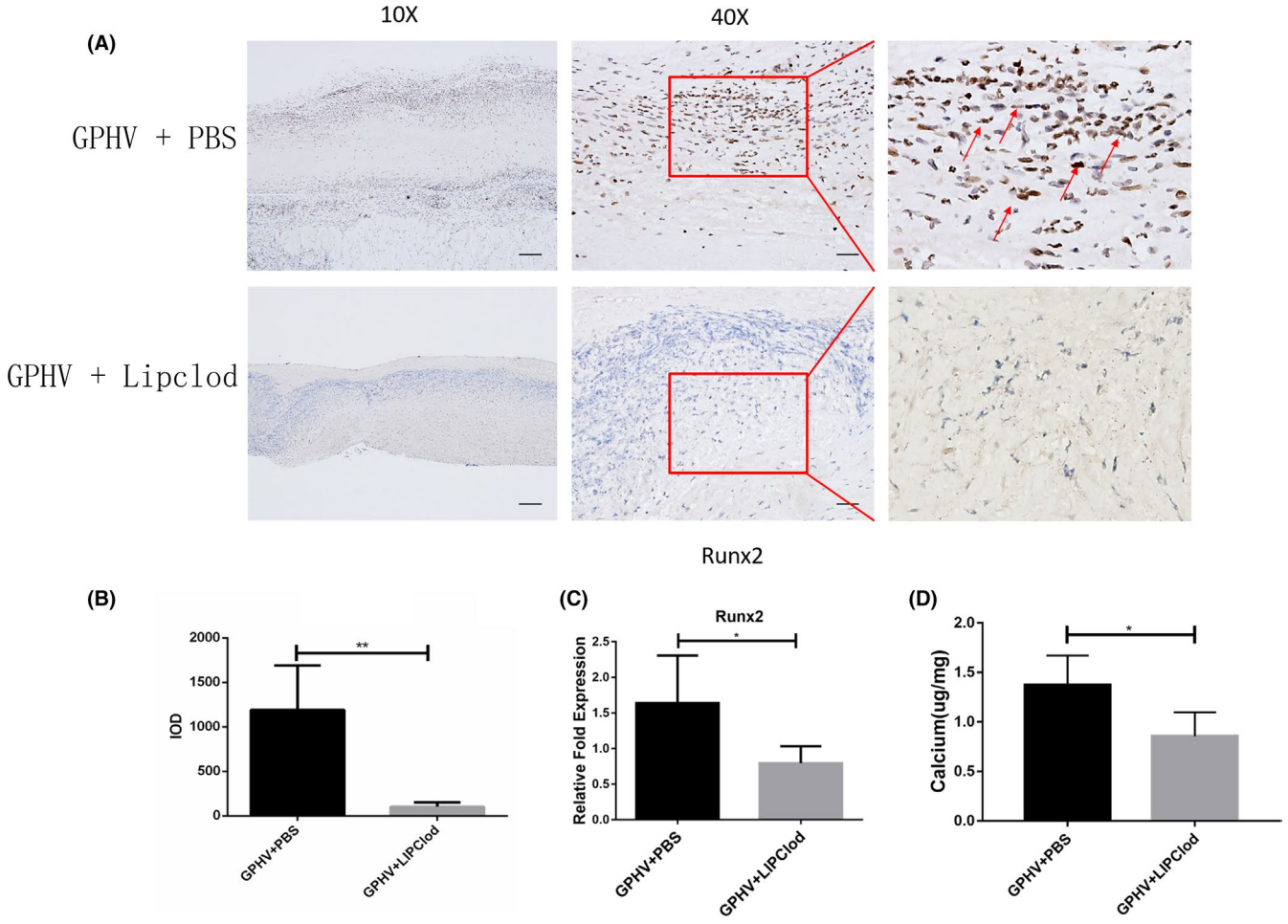

FIGURE 6 Histological characterization of calcification of GPHV in an in vivo implantation subdermal mouse model over a four-week period. (A, B) Representative images of the immunohistochemical staining and quantification data show that liposomal treatment significantly decreased Runx2 expression in GPHV compared with PBS liposomes. (C) Polymerase chain reaction (PCR) expression levels of Runx2 varied between groups (n = 5 per group, $^{*}p < .05$; $^{***}p < .001$, Student's t test). (D) Quantitative calcium content comparisons between studied groups

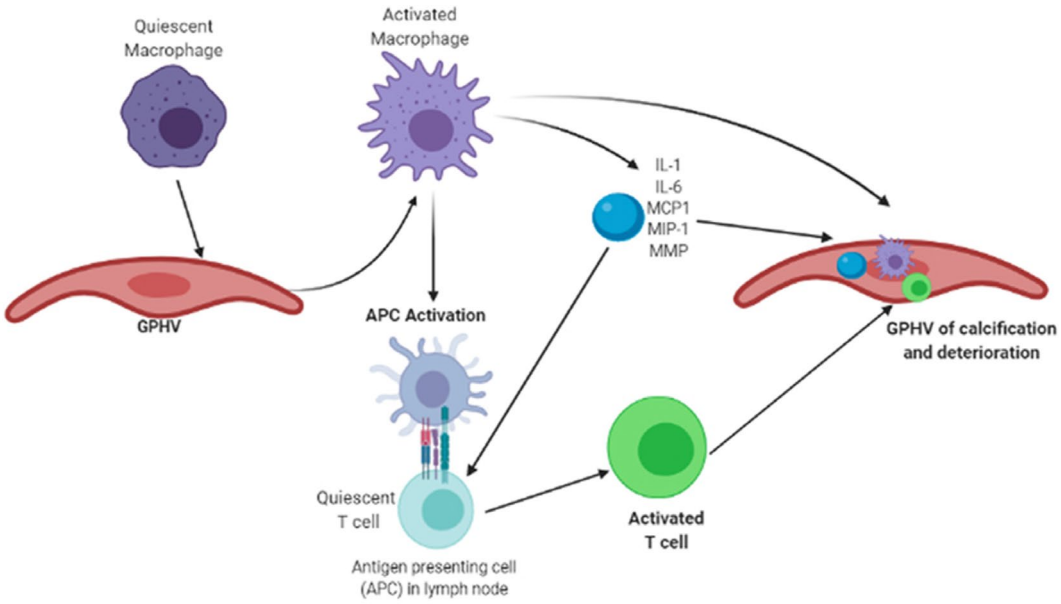

FIGURE 7 Macrophages can induce valve degradation and calcification by secreting cytokines and MMPs, and can also increase $CD3^{+}$ T-cell activation, thus increasing the infiltration of T cells into GBHV. Once activated, stationary T cells can differentiate into cytotoxic T cells and secrete cytokines mediating valve degradation

evaluate the side effects of the macrophage elimination. It is reported that the $AlCl_3$ pretreatment of elastin leads to inhibition of MMP-mediated degradation of elastin.[30] In turn, this leads to the inhibition of elastin-oriented calcification in a rat subdermal implantation model as well as in sheep mitral valve replacement studies.[30,31] Another research also reported that the inhibition of the MMP activity could also reduce calcium accumulation in rodent models of aortic calcification.[32]

The other beneficial effect of the Lipclod treatment was related to reduced extent of calcification. Apart from the fact that Lipclod treatment caused reduced calcium deposition within GPHV, the lower expression of early osteoblast marker RUNX2, ALP and OPN (Supplementary material) was also witnessed in GPHV compared with controls. One possible explanation was that macrophages and osteoclasts could secrete chemotactic signals, including IL-1a, IL-6, and MCP-1, that attracted pre-osteoblasts in inflammatory microenvironments which would finally lead to osteoblast marker expression.[33-35]

5 | CONCLUSIONS

In this study, we have proved that the clearance of macrophages by clodronate liposomes can significantly reduce the infiltration of inflammatory cells and other proinflammatory cytokines on GPHV, as well as the secretion of MMP-2 and MMP-9. The clearance of macrophage could also reduce calcium deposition and osteoblast marker RUNX2, ALP and OPN expression, thus improving the degeneration and calcification of the GPHV (Figure 7). This study establishes a theoretical basis for the improvement of GBHVs and targeted drug therapy of bioprosthetic heart valve deterioration.

ACKNOWLEDGEMENTS

This work was supported by the National Key Research and Development Program (No. 2016YFA0101100) and the National Natural Science Foundation of China (82001701). No author has an actual or perceived conflict of interest with the contents of this article.

ETHICS STATEMENT

The study was approved by the Ethics Committee of Tongji Medical College of Huazhong University of Science and Technology (IORG No. IORG0003571).

AUTHORSHIP CONTRIBUTIONS

Participated in research design: Zongtao Liu, Yixuan Wang, Nianguo Dong, Fei Li. Conducted Experiments: Zongtao Liu, Yixuan Wang, Fei Xie. Performed data analysis: Zongtao Liu, Yixuan Wang, Fei Li. Contributed to the Writing of the manuscript: Zongtao Liu, Yixuan Wang, Nianguo Dong, Fei Li, Xing Liu.

DATA AVAILABILITY STATEMENT

The data that support the findings of this study are available from the corresponding author upon reasonable request.

ORCID

Nianguo Dong https://orcid.org/0000-0003-1558-4523

REFERENCES

1. Siddiqui RF, Abraham JR, Butany J. Bioprosthetic heart valves: modes of failure. *Histopathology*. 2009;55(2):135-144.
2. Bre LP, McCarthy R, Wang W. Prevention of bioprosthetic heart valve calcification: strategies and outcomes. *Curr Med Chem*. 2014;21(22):2553-2564.
3. Sun JC, Davidson MJ, Lamy A, Eikelboom JW. Antithrombotic management of patients with prosthetic heart valves: current evidence and future trends. *Lancet*. 2009;374(9689):565-576.
4. Ochi A, Cheng K, Zhao B, Hardikar AA, Negishi K. Patient risk factors for bioprosthetic aortic valve degeneration: a systematic review and meta-analysis. *Heart Lung Circ*. 2020;29(5):668-678.
5. Grabenwoger M, Fitzal F, Gross C, et al. Different modes of degeneration in autologous and heterologous heart valve prostheses. *J Heart Valve Dis*. 2000;9(1):104-109; discussion 10–1.
6. Shetty R, Pibarot P, Audet A, et al. Lipid-mediated inflammation and degeneration of bioprosthetic heart valves. *Eur J Clin Invest*. 2009;39(6):471-480.
7. Galli D, Manuguerra R, Monaco R, et al. Understanding the structural features of symptomatic calcific aortic valve stenosis: A broad-spectrum clinico-pathologic study in 236 consecutive surgical cases. *Int J Cardiol*. 2017;228:364-374.
8. Soini Y, Satta J, Maatta M, Autio-Harmainen H. Expression of MMP2, MMP9, MT1-MMP, TIMP1, and TIMP2 mRNA in valvular lesions of the heart. *J Pathol*. 2001;194(2):225-231.
9. Kaden JJ, Dempfle C-E, Grobholz R, et al. Inflammatory regulation of extracellular matrix remodeling in calcific aortic valve stenosis. *Cardiovasc Pathol*. 2005;14(2):80-87.
10. Satta J, Oiva J, Salo T, et al. Evidence for an altered balance between matrix metalloproteinase-9 and its inhibitors in calcific aortic stenosis. *Ann Thorac Surg*. 2003;76(3):681-688.discussion 8.
11. Simionescu A, Simionescu D, Deac R. Biochemical pathways of tissue degeneration in bioprosthetic cardiac valves. The role of matrix metalloproteinases. *ASAIO J*. 1996;42(5):M561-M567.
12. Ylitalo R, Syvala H, Tuohimaa P, Ylitalo P. Suppression of immunoreactive macrophages in atheromatous lesions of rabbits by clodronate. *Pharmacol Toxicol*. 2002;90(3):139-143.
13. Cohen-Sela E, Dangoor D, Epstein H, et al. Nanospheres of a bisphosphonate attenuate intimal hyperplasia. *J Nanosci Nanotechnol*. 2006;6(9–10):3226-3234.
14. Manji RA, Zhu LF, Nijjar NK, et al. Glutaraldehyde-fixed bioprosthetic heart valve conduits calcify and fail from xenograft rejection. *Circulation*. 2006;114(4):318-327.
15. Neethling W, Brizard C, Firth L, Glancy R. Biostability, durability and calcification of cryopreserved human pericardium after rapid glutaraldehyde-stabilization versus multistep ADAPT(R) treatment in a subcutaneous rat model. *Eur J Cardiothorac Surg*. 2014;45(4):e110-e117.
16. Weisser SB, van Rooijen N, Sly LM. Depletion and reconstitution of macrophages in mice. *J Vis Exp*. 2012;66:4105.
17. Manji RA, Lee W, Cooper DKC. Xenograft bioprosthetic heart valves: past, present and future. *Int J Surg*. 2015;23(Pt B):280-284.
18. Parisi V, Leosco D, Ferro G, et al. The lipid theory in the pathogenesis of calcific aortic stenosis. *Nutr Metab Cardiovasc Dis*. 2015;25(6):519-525.
19. Olszowska M. Pathogenesis and pathophysiology of aortic valve stenosis in adults. *Pol Arch Med Wewn*. 2011;121(11):409-413.
20. Ardans JA, Economou AP, Martinson JM Jr, Zhou M, Wahl LM. Oxidized low-density and high-density lipoproteins regulate the production of matrix metalloproteinase-1 and -9 by activated monocytes. *J Leukoc Biol*. 2002;71(6):1012-1018.
21. Tayebjee MH, Lip GY, MacFadyen RJ. Matrix metalloproteinases in coronary artery disease: clinical and therapeutic implications and pathological significance. *Curr Med Chem*. 2005;12(8):917-925.
22. Okamura K, Chiba C, Iriyama T, et al. Antigen depressant effect of glutaraldehyde for aortic heterografts with a valve, with special reference to a concentration right fit for the preservation of grafts. *Surgery*. 1980;87(2):170-176.
23. Villa ML, De Biasi S, Pilotto F. Residual heteroantigenicity of glutaraldehyde-treated porcine cardiac valves. *Tissue Antigens*. 1980;16(1):62-69.
24. Simionescu DT. Prevention of calcification in bioprosthetic heart valves: challenges and perspectives. *Expert Opin Biol Ther*. 2004;4(12):1971-1985.
25. Calin MV, Manduteanu I, Dragomir E, et al. Effect of depletion of monocytes/macrophages on early aortic valve lesion in experimental hyperlipidemia. *Cell Tissue Res*. 2009;336(2):237-248.
26. Schussler O, Shen M, Shen L, Carpentier SM, Kaveri S, Carpentier A. Effect of human immunoglobulins on the immunogenicity of porcine bioprostheses. *Ann Thorac Surg*. 2001;71(5 Suppl):S396-400.
27. Human P, Zilla P. Characterization of the immune response to valve bioprostheses and its role in primary tissue failure. *Ann Thorac Surg*. 2001;71(5 Suppl):S385-S388.
28. van Rooijen N, van Kesteren-Hendrikx E. Clodronate liposomes: perspectives in research and therapeutics. *J Liposome Res*. 2002;12(1–2):81-94.
29. van Rooijen N, Hendrikx E. Liposomes for specific depletion of macrophages from organs and tissues. *Methods Mol Biol*. 2010;605:189-203.
30. Bailey M, Xiao H, Ogle M, Vyavahare N. Aluminum chloride pretreatment of elastin inhibits elastolysis by matrix metalloproteinases and leads to inhibition of elastin-oriented calcification. *Am J Pathol*. 2001;159(6):1981-1986.
31. Lee JS, Basalyga DM, Simionescu A, Isenburg JC, Simionescu DT, Vyavahare NR. Elastin calcification in the rat subdermal model is accompanied by up-regulation of degradative and osteogenic cellular responses. *Am J Pathol*. 2006;168(2):490-498.
32. Qin X, Corriere MA, Matrisian LM, Guzman RJ. Matrix metalloproteinase inhibition attenuates aortic calcification. *Arterioscler Thromb Vasc Biol*. 2006;26(7):1510-1516.
33. Vasconcelos DP, Costa M, Amaral IF, Barbosa MA, Aguas AP, Barbosa JN. Modulation of the inflammatory response to chitosan through M2 macrophage polarization using pro-resolution mediators. *Biomaterials*. 2015;37:116-123.
34. Li G, Qiao W, Zhang W, Li F, Shi J, Dong N. The shift of macrophages toward M1 phenotype promotes aortic valvular calcification. *J Thorac Cardiovasc Surg*. 2017;153(6):1318-27 e1.
35. Zheng D, Zang Y, Xu H, et al. MicroRNA-214 promotes the calcification of human aortic valve interstitial cells through the acceleration of inflammatory reactions with activated MyD88/NF-kappaB signaling. *Clin Res Cardiol*. 2019;108(6):691-702.

SUPPORTING INFORMATION

Additional supporting information may be found online in the Supporting Information section.

How to cite this article: Liu Z, Wang Y, Xie F, Liu X, Li F, Dong N. Elimination of macrophages reduces glutaraldehyde-fixed porcine heart valve degeneration in mice subdermal model. *Pharmacol Res Perspect*. 2021;9:e00716. https://doi.org/10.1002/prp2.716